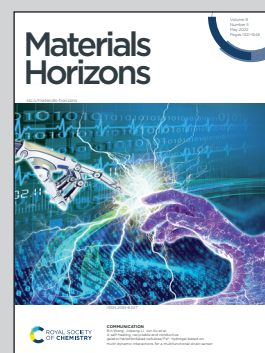


Showcasing research from Professor Shi Liu's Multiscale Materials Modeling Laboratory at Westlake University, Zhejiang, China.

On-demand quantum spin Hall insulators controlled by two-dimensional ferroelectricity

We propose a new class of quantum materials, type-II two-dimensional ferroelectric topological insulators (2DFETIs), that has the band topology directly coupled to the ferroelectricity, thus allowing non-volatile and on-off switching of quantum spin Hall states. The 2DFETI-based topological memristor, combining the advantages of topological insulators, ferroelectrics, and two-dimensional materials, may hold the promise for energy-efficient, high-density synaptic electronics and neuromorphic systems.

As featured in:



See Jian Li, Shi Liu *et al.*,
Mater. Horiz., 2022, **9**, 1440.

Cite this: *Mater. Horiz.*, 2022, 9, 1440Received 15th March 2022,
Accepted 6th April 2022

DOI: 10.1039/d2mh00334a

rsc.li/materials-horizons

On-demand quantum spin Hall insulators controlled by two-dimensional ferroelectricity†

Jiawei Huang,^{ab} Xu Duan,^{bc} Sunam Jeon,^d Youngkuk Kim,^e Jian Zhou,^f Jian Li^{*,bg} and Shi Liu^{*,bg}

We propose a new class of quantum materials, type-II two-dimensional ferroelectric topological insulators (2DFETIs), which allow non-volatility and an on-off switch of quantum spin Hall states. A general strategy is developed to realize type-II 2DFETIs using only topologically trivial 2D ferroelectrics. The built-in electric field arising from the out-of-plane polarization across the bilayer heterostructure of 2D ferroelectrics enables robust control of the band gap size and band inversion strength, which can be utilized to manipulate the topological phase transitions on-demand. Using first-principles calculations with hybrid density functionals, we demonstrate that a series of bilayer heterostructures are type-II 2DFETIs characterized with a direct coupling between the band topology and polarization state. We propose a few 2DFETI-based quantum electronics, including domain-wall quantum circuits and topological memristors.

Band topology and ferroelectricity, two extensively studied properties of bulk insulators representing two distinct “ordered states”, can manifest themselves in two dimensions. Graphene as the first discovered two-dimensional (2D) material¹ is also the first predicted 2D topological insulator (TI) characterized by counter-propagating edge currents with opposite spin polarization and an insulating interior.² A 2D TI is also called a quantum spin Hall (QSH) insulator due to its quantized edge

New concepts

By analogy with type-I multiferroics in which different origins of magnetism and ferroelectricity lead to weak magnetoelectric coupling, most reported two-dimensional ferroelectric topological insulators (2DFETIs) are type-I by nature: the switching of ferroelectric polarization has no control over the nature of band topology. Here, we propose a new class of quantum materials, type-II 2DFETIs, which have the band topology directly coupled to the ferroelectricity, thus allowing non-volatility and an on-off switch of quantum spin Hall states. The design principle for type-II 2DFETIs is demonstrated using van der Waals bilayer heterostructures comprising only trivial 2D FEs: the built-in electric field associated with the out-of-plane polarization is utilized to drive the band inversion needed for topological phase transition. Several type-II 2DFETI-based quantum electronics are proposed, including domain-wall quantum electrical circuits and non-volatile topological memristors for synaptic electronics and neuromorphic systems.

conductance ($2e^2/h$ where e is the elementary charge and h is Planck's constant). Finding 2D TIs with large band gaps for room-temperature applications remains an actively pursued goal.^{3–6}

Ferroelectrics (FEs) with inversion symmetry breaking often exhibit a strong size effect that the spontaneous polarization is diminished with reduced dimensionality due to the depolarization field from the incomplete screening of surface charges.⁷ More recently, facilitated by first-principles calculations based on density functional theory (DFT), a range of 2D FEs were discovered followed by confirming experiments.^{8–12} Specifically, α -In₂Se₃ exhibits out-of-plane electric polarization,^{9,13} a feature beneficial for practical device applications and high-density integrations. As the surfaces of 2D materials do not suffer from dangling bonds, it is feasible to stack different 2D sheets to construct van der Waals (vdW) heterostructures in a precisely controlled layering sequence less impacted by the lattice mismatch.^{14–16}

A 2D material system with both ferroelectric and topological orders, referred to as a 2D ferroelectric topological insulator (2DFETI), remains rarely reported other than some chance

^a Zhejiang University, Hangzhou, Zhejiang 310058, P. R. China

^b Department of Physics, School of Science, Westlake University, Hangzhou, Zhejiang 310024, China. E-mail: lijian@westlake.edu.cn, liushi@westlake.edu.cn

^c Fudan University, Shanghai 200433, China

^d Department of Energy Science, Sungkyunkwan University, Suwon 16419, Korea

^e Department of Physics, Sungkyunkwan University, Suwon 16419, Korea

^f Center for Alloy Innovation and Design, State Key Laboratory for Mechanical Behavior of Materials, Xi'an Jiaotong University, Xi'an 710049, China

^g Institute of Natural Sciences, Westlake Institute for Advanced Study, Hangzhou, Zhejiang 310024, China

† Electronic supplementary information (ESI) available: Computational details, band bending diagram, generic four-band model, band structures and \mathbb{Z}_2 calculations, HSE06 vs. PBE band structures, layer-resolved density of states, phonon spectra, *ab initio* molecular dynamics simulations, and switching barriers. See DOI: <https://doi.org/10.1039/d2mh00334a>

discovery.^{17–21} The common strategy is to induce the breaking of the inversion symmetry in a known 2D TI either by functionalizing it covalently¹⁷ or placing it next to a known 2D FE.^{19,20} The requirement of a 2D TI limits the applicability of such a strategy. Moreover, a mere coexisting of ferroic and topological orders does not guarantee a strong coupling between topological and polarization states. For example, ligand-CH₂OH-functionalized bismuth monolayer (BiCH₂OH)¹⁷ and fluorinated methyl-functionalized bismuthine (Bi₂C₂H_{6–x}F_x),¹⁸ though possessing both ferroelectricity and nontrivial band topology, are unlikely to realize an on–off switch of QSH states through polarization reversal. By analogy with type-I multiferroics in which different origins of magnetism and ferroelectricity lead to weak magnetoelectric coupling,^{22,23} most reported 2DFETIs can also be called type-I by nature: the switching of ferroelectric polarization has no control over the nature of the band topology.^{17,18,21} The challenge to couple ferroelectric and topological orders strongly is partly due to the “band gap dilemma”:²⁴ TIs are often narrow-gap semiconductors with a band gap determined by the strength of spin-orbit coupling (SOC) whereas archetypal FEs such as transition metal perovskites are mostly wide-band-gap insulators with the gap size dictated by the electronegativity difference between oxygen and transition metals. Unlike bulk FEs in 3D, many 2D FEs are semiconductors with moderate band gaps,¹³ thus being better suited for the coexistence of the topological order.

Here we propose a design principle for the realization of 2DFETIs in bilayer heterostructures comprising only trivial 2D FEs. The ability to create nontrivial quantum materials using trivial building blocks broadens the material design space. Moreover, the band topology is directly coupled to the polarization state: the nonvolatile QSH states can be fully switched on and off *via* voltage, giving rise to what we call type-II 2DFETIs. The key requirement for the constituent 2D FEs is the presence of out-of-plane polarization (P_{OP}). For a free-standing monolayer, the polarization-bound charges on the two surfaces create a depolarization field (E_d) that runs against the polarization. As a result, the valence band maximum (VBM) is located on the negatively-charged (Q^-) surface, while the conduction band minimum (CBM) is on the positively-charged (Q^+) surface (Fig. 1a). A heuristic way to understand such “band bending” is that electrons close to the Q^- surface are at a high energy level (thus being at VBM) because of the Coulomb repulsion. The band diagram of a 2D FE with P_{OP} resembles that of an unbiased p–n junction, and E_d across the monolayer is similar to the electric field confined to the depletion region around the junction interface (see Fig. S1 in ESI†). Since the potential step ($\Delta\Phi$) scales with P_{OP} , one might expect the crossover of VBM and CBM given a sufficiently large P_{OP} . However, such band inversion is less likely to happen in a monolayer as the system would become metallic at the crossover, providing more free carriers for surface charge compensation, thus reducing E_d and band bending. Therefore, a 2D FE by itself has a tendency to avoid the band inversion by maintaining an optimal trade-off between imperfect screening and a minimal necessary band bending.²⁵ We note that homogenous bilayer or trilayer 2D FEs

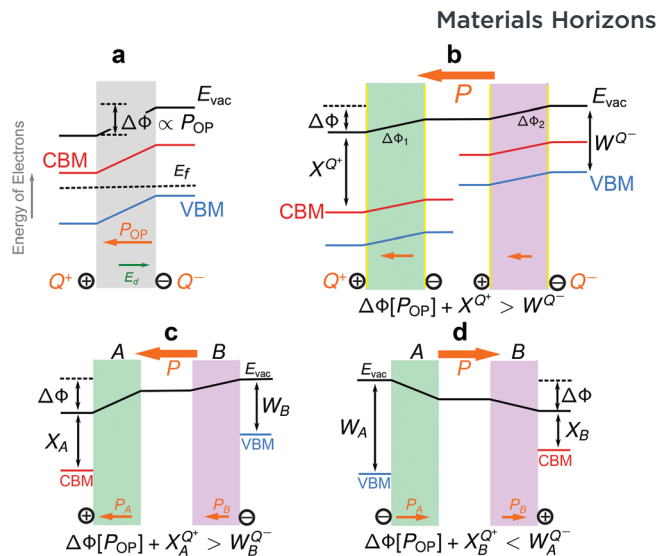


Fig. 1 Design principle for type-II two-dimensional ferroelectric topological insulators. Band bending in (a) monolayer 2D ferroelectrics and (b) bilayer heterostructures consisting of two different 2D ferroelectrics with out-of-plane polarization (P_{OP}). The potential step ($\Delta\Phi$) across the monolayer is due to the depolarization field (E_d) arising from the incomplete screening of surface charges associated with P_{OP} . The band bending is similar to what occurred at the depletion region of a p–n junction. When ignoring the interlayer charge transfer, the bilayer heterostructure can be approximated as parallel plate capacitor (yellow solid lines), and the total potential step ($\Delta\Phi = \Delta\Phi_1 + \Delta\Phi_2$) does not depend on the interlayer distance because of the zero field in the interlayer region according to Gauss’s law. The band inversion can be controlled by the switching of P_{OP} . (c) Potential topological insulator phase due to band inversion. (d) Trivial insulator phase with uninverted bands.

could exhibit band inversion; but the reversal of the polarization cannot change the band topology thus rendering them type-I 2DFETIs.

In contrast, a bilayer heterostructure made of two different 2D FEs (Fig. 1b) allows for a band inversion process when the following condition is satisfied:

$$\Delta\Phi[P_{OP}] + X^{Q^+} > W^{Q^-} \quad (1)$$

where X^{Q^+} is the electron affinity of the Q^+ surface and W^{Q^-} is the work function of the Q^- surface of the heterostructure, respectively. The superscripts Q^+ and Q^- label the two outmost surfaces, belonging to two different monolayers, respectively. It is evident from Fig. 1b that $E_{VBM} = -W^{Q^-}$ and $E_{CBM} = -(\Delta\Phi + X^{Q^+})$ relative to the vacuum level and eqn (1) naturally leads to $E_{CBM} < E_{VBM}$ and thus a band inversion. According to the celebrated Neumann–Wigner theorem,²⁶ the presence of crossing between two bands often demands a symmetry-related protection (*e.g.*, mirror symmetry). For a generic system without special crystalline symmetries, the SOC will then lead to a double group system where a gap generically opens between the valence and conduction bands, likely resulting in a QSH state. Because X^{Q^+} and W^{Q^-} are coming from two different materials, a 2DFETI can be realized by selecting one monolayer with large X and another monolayer with small W .

Furthermore, by choosing a pair of 2D FEs (labeled as *A* and *B*, respectively), satisfying

$$\Delta\Phi[P_{\text{OP}}] + X_{\text{A}}^{Q^+} > W_{\text{B}}^{Q^-}; \Delta\Phi[P_{\text{OP}}] + X_{\text{B}}^{Q^+} < W_{\text{A}}^{Q^-}, \quad (2)$$

we can ensure that the configuration with *P* pointing from *B* to *A* has band inversion (Fig. 1c) while the other configuration with *P* pointing from *A* to *B* is a normal insulator (Fig. 1d), creating a pair of topologically different, non-volatile states in the absence of external electric fields. This can be accomplished by choosing *A* with large *X* and *W* whereas *B* with small *W* and *X*. This design principle can lead to a type-II 2DFETI that has the nature of band topology directly coupled to the direction of ferroelectric polarization.

An advantage of the proposed type-II 2DFETI is the “on-demand” topological quantum phase transition. For a band inversion process driven by SOC, the inversion strength $\lambda = E_{\text{VBM}} - E_{\text{CBM}}$ is intrinsically limited by the atomic numbers of heavy elements contributing to the states near E_{F} . In comparison, the inversion strength of the proposed bilayer system is directly coupled to the potential step $\Delta\Phi$ across the heterostructure, $\lambda = \Delta\Phi + X^{Q^+} - W^{Q^-}$. In general, *X* and *W* are less sensitive to the change of polarization for a given material. When ignoring the interlayer charge transfer, the bilayer can be approximated as parallel plate capacitors (illustrated as yellow solid lines in Fig. 1b), and $\Delta\Phi$ does not depend on the interlayer distance because the electric field in the interlayer region is zero according to Gauss’s law. Therefore, $\Delta\Phi$ almost singularly depends on P_{OP} (and thus E_{d}) of constituent 2D FEs. By applying external electric/stress fields to vary P_{OP} , the magnitude of λ can thus be tuned nearly continuously. This implies access to multiple electronic band configurations that are effectively characterized by the magnitude of λ and can belong to distinct topological phases. Using a generic model (see details in Section III, ESI†), we explore the evolution of the

band topology with increasing value of λ and identify successive phase transitions associated with two band inversion events, occurring at the Γ -point and then non-high-symmetry points in the Brillouin zone. The two quantum phase transition points (band gap $E_{\text{g}} = 0$, see Fig. 2a) separate trivial, nontrivial, and trivial phases, respectively, as verified by Wilson loop calculations (Fig. 2b).

The single-equation design principle that depends on only three basic material parameters serves as useful guidance for the search of realistic material systems. Below, using bilayer heterostructures made of α -III₂-VI₃-type 2D FEs as model systems, we demonstrate the feasibility of the design principle based on DFT calculations. A typical α -III₂-VI₃-type 2D FE in the space group of *P3m1* comprises five atomic planes in the order of VI-III-VI-III-VI, in which the central layer is displaced relative to the top and bottom III-VI layers, resulting in out-of-plane polarization (P_{OP} , Fig. 3a). Phonon spectrum calculations in previous studies confirmed that α -III₂-VI₃-type 2D FEs such as α -In₂S₃, α -In₂Se₃, α -In₂Te₃, and α -Ga₂S₃ are all dynamically stable without an imaginary frequency in the phonon spectra (Fig. S18, ESI†).¹³ It is a common practice for computational materials by design to gauge the stability of a new material based on the phonon spectrum that captures the intrinsic stability.^{5,27–29} We note that the 2D ferroelectricity in monolayer α -In₂Se₃ was first predicted based on DFT calculations¹³ and later confirmed experimentally.^{9,30–32} More recently, nanoflakes of α -Ga₂S₃, a homologous compound of α -In₂Se₃, have been synthesized.³³ These results support that the absence of an imaginary frequency in the phonon spectrum is a meaningful indicator of material synthesizability. It is thus plausible that other α -III₂-VI₃-type 2D FEs such as α -In₂S₃ and α -In₂Te₃ could be synthesized as well, and designed bilayer systems in this work are equally plausible. It was proposed that *ab initio* molecular dynamics (AIMD) can be used to further confirm structural stability.³⁴ We performed additional AIMD

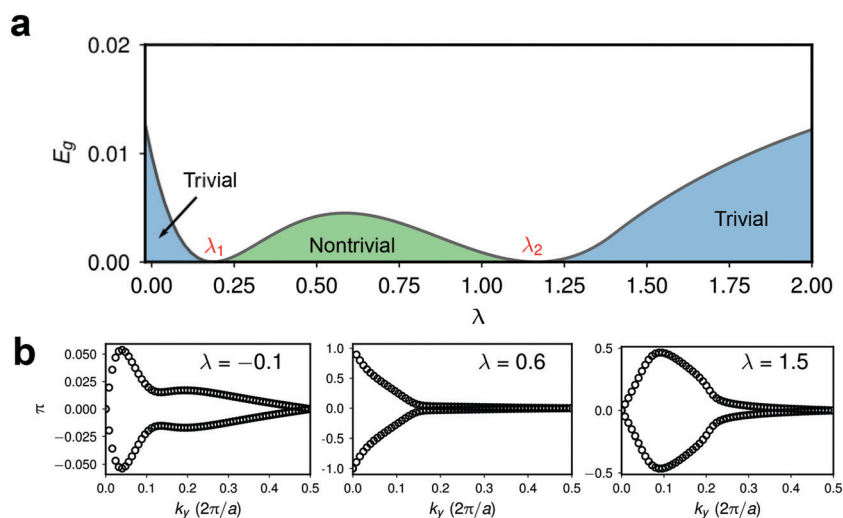


Fig. 2 Successive trivial-nontrivial-trivial phase transitions driven by the strength (λ) of band inversion. The generic phase diagram is obtained using an extended BHZ model on a two-dimensional square lattice. (a) Numerically obtained band gap as a function of λ . (b) Wilson loop calculations for three different phases.

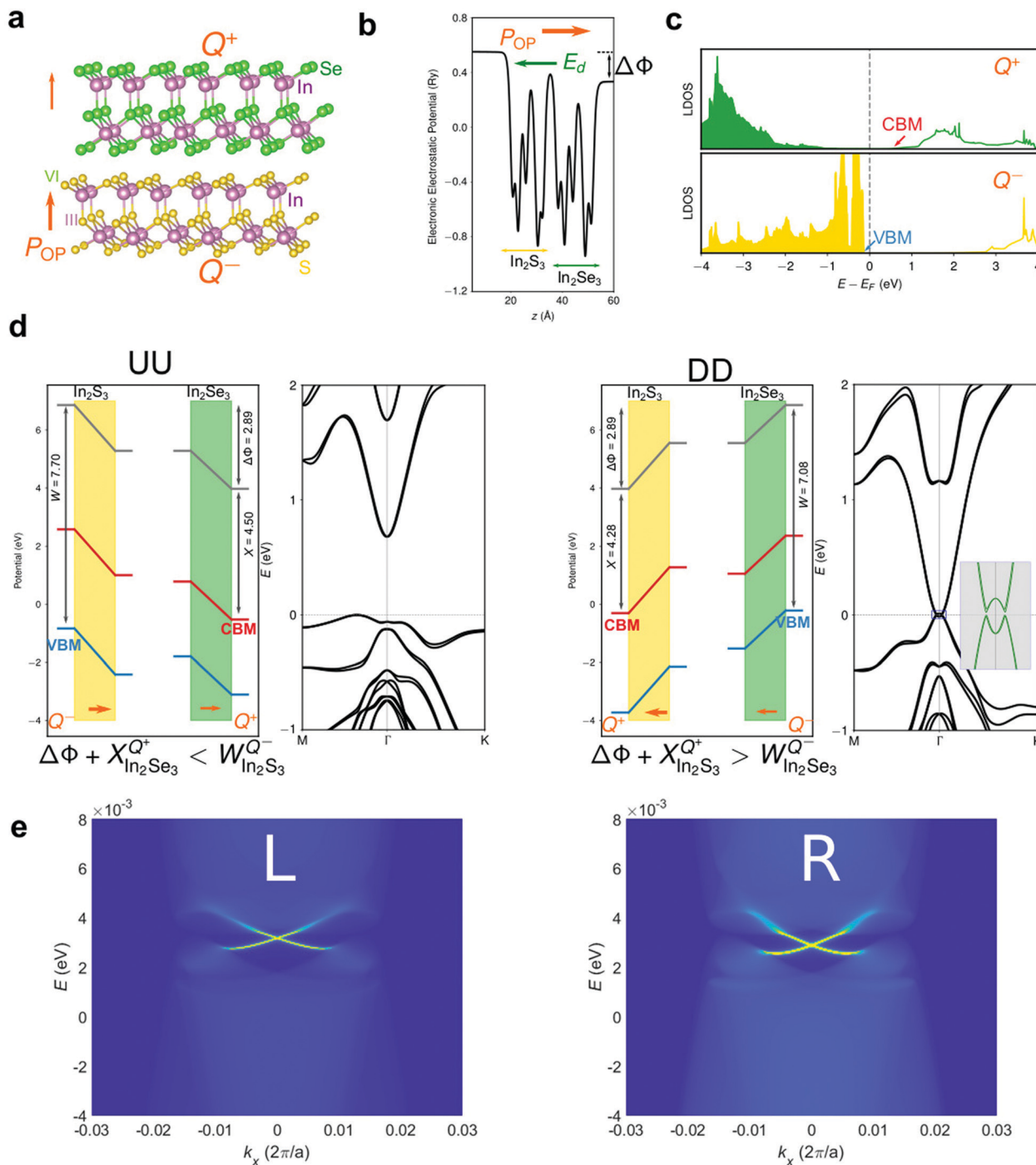


Fig. 3 Electronic structures of $\text{In}_2\text{Se}_3/\text{In}_2\text{S}_3$ bilayer heterostructures. (a) Atomic structures of the $\text{In}_2\text{Se}_3/\text{In}_2\text{S}_3$ bilayer heterostructure of the UU configuration. (b) Electronic electrostatic potential of the UU configuration and (c) layer-resolved local density of states (LDOS) for Q^+ and Q^- surfaces computed with HSE06. The dipole correction method⁴⁹ is employed to compute $\Delta\Phi$, while the supercell remains periodic in all three directions. The potential step across the bilayer and the locations of the VBM and CBM are consistent with Fig. 1d. (d) HSE06 band structures of UU and DD configurations. (e) Spectral functions at the edges of the DD configuration. Because of in-plane asymmetry; the left (L) and right (R) edges have relatively shifted Dirac cones.

calculations for $\alpha\text{-In}_2\text{S}_3$, $\alpha\text{-In}_2\text{Te}_3$, and some bilayer systems and confirmed their stability at finite temperatures (Fig. S19, ESI[†]). Moreover, recent experimental realizations of sliding ferroelectricity³⁵ in 2D vdW materials using nonferroelectric 2D materials such as $h\text{-BN}$ have substantially broadened the

candidates of 2D FEs with out-of-plane polarization,^{36,37} indicating a wide applicability of the proposed design principle for type-II 2DFETs.

The vdW heterostructures are fully optimized using a generalized gradient approximation of the Perdew–Burke–

Ernzerhof (PBE) type with Grimme dispersion corrections as implemented in QUANTUM ESPRESSO^{38,39} (see more details in ESI†). To address the well-known issue of band gap underestimation of (semi-)local DFT such as PBE, we compute the electronic properties (*e.g.*, X and W) with the Heyd–Scuseria–Ernzerhof (HSE) hybrid density functional⁴⁰ for some representative systems. The HSE06 band structure with SOC is obtained *via* Wannier interpolation⁴¹ using Wannier90⁴² interfaced with QUANTUM ESPRESSO. To recognize the topological state of this system, we obtain the \mathbb{Z}_2 topological index by calculating the Wilson loop spectrum using the maximum localized Wannier function tight-binding Hamiltonians constructed with Wannier90. The boundary spectral function of a 2D TI is computed using the boundary Green function technique in a semi-infinite geometric setting such that boundary states can be easily identified even for systems with a small gap as the local (boundary) spectral weight is dominated by the contribution from boundary states. In our calculations, the edge is created by imposing an open boundary condition for certain unit cells, and the width is infinite because of the semi-infinite geometry.

We focus on the bilayer heterostructure made of monolayer In_2Se_3 and In_2S_3 . The monolayer properties calculated with HSE06 are as follows: $W_{\text{In}_2\text{Se}_3} = 7.08$ eV, $X_{\text{In}_2\text{Se}_3} = 4.50$ eV, $\Delta\Phi_{\text{In}_2\text{Se}_3} = 1.31$ eV and $W_{\text{In}_2\text{S}_3} = 7.70$ eV, $X_{\text{In}_2\text{S}_3} = 4.28$ eV, and $\Delta\Phi_{\text{In}_2\text{S}_3} = 1.58$ eV. The configuration with out-of-plane polarization pointing from In_2S_3 (Q^- surface) to In_2Se_3 (Q^+ surface) is denoted as UU (up-up, Fig. 3b). The computed electronic electrostatic potential across the UU bilayer (Fig. 3b) is consistent with the design principle illustrated in Fig. 1d. The layer-resolved local density of states (Fig. 3c) confirm that the VBM and CBM are located at Q^- and Q^+ surfaces, respectively. According to eqn (2), the UU configuration is a normal insulator as $\Delta\Phi_{\text{In}_2\text{S}_3} + \Delta\Phi_{\text{In}_2\text{Se}_3} + X_{\text{In}_2\text{Se}_3}^{Q^+} < W_{\text{In}_2\text{S}_3}^{Q^-}$. In comparison, the configuration with a reversed polarization, denoted as DD (down-down), has In_2S_3 being the Q^+ surface and In_2Se_3 being the Q^- surface. Then the band inversion can occur because $\Delta\Phi_{\text{In}_2\text{S}_3} + \Delta\Phi_{\text{In}_2\text{Se}_3} + X_{\text{In}_2\text{S}_3}^{Q^+} > W_{\text{In}_2\text{Se}_3}^{Q^-}$. The HSE06 band structures as shown in Fig. 3d for the UU and DD configurations further corroborate the above analysis. The UU configuration is a trivial insulator with an indirect band gap of 0.68 eV. As for the DD configuration, the inverted gap at Γ is evident in

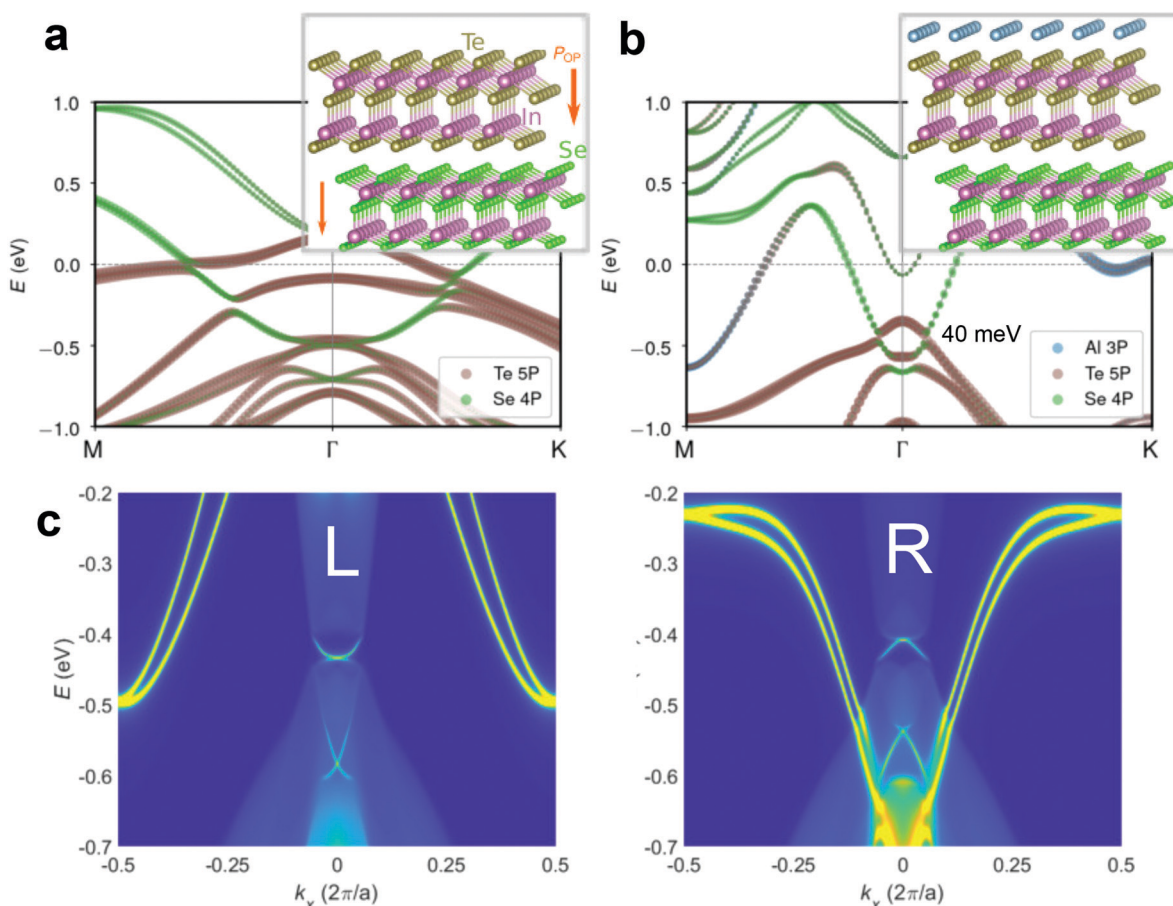


Fig. 4 : Electronic structures of $\text{In}_2\text{Te}_3/\text{In}_2\text{Se}_3$ vdW heterostructures. Atomic orbital-resolved band structures of (a) $\text{In}_2\text{Te}_3/\text{In}_2\text{Se}_3$ bilayer and (b) $\text{Al}/\text{In}_2\text{Te}_3/\text{In}_2\text{Se}_3$ trilayer of the DD configuration. The insets show the structures of heterostructures. (c) Spectral functions at the edges of $\text{Al}/\text{In}_2\text{Te}_3/\text{In}_2\text{Se}_3$ trilayer. Because of the break of inversion symmetry in plane, the left (L) and right (R) edges may acquire positive and negative bound charges, leading to shifted Dirac cones.

the band structure, and small anticrossing gaps (≈ 2 meV) open at generic k points away from Γ . We note here that the band gap size can be further enhanced (see discussions below). Calculations of the \mathbb{Z}_2 invariant using the Wilson loop approach confirm that the DD configuration is indeed in the QSH insulator phase. As a consequence, topological edge states occur at the boundaries of these samples, which can be clearly seen from the boundary spectral functions shown in Fig. 3e. These results from HSE06 calculations support the proposed design principle for the realization of type-II 2DFETIs that have the topological quantum state originating from the ferroelectricity. Similarly, we find that a number of bilayer heterostructures are type-II 2DFETIs based on PBE calculations, *i.e.*, the DD configurations of $\text{Al}_2\text{Te}_3/\text{Al}_2\text{Se}_3$ and $\text{Al}_2\text{Te}_3/\text{In}_2\text{S}_3$. The non-trivial band topologies of these systems are confirmed by \mathbb{Z}_2 calculations (see ESI†).

The central quantity of the design principle proposed in this work is P_{OP} and associated E_{d} , which in principle can be continuously tuned. In experimental realizations, we suggest that various factors such as the dielectric constants of substrates, unintentional doping due to chemicals used in the device fabrication process, and in-plane strains induced by the lattice mismatch can serve as knobs to obtain precise control of E_{d} and λ . For example, one can use another layer of semiconducting 2D material or a substrate to partially screen the surface charges of the bilayer, thus setting the magnitude of E_{d} and λ to the desired value. We now offer an example to demonstrate the highly configurable band topology by tuning the strength of λ . The generic phase diagram shown in Fig. 2b suggests that a too large value of λ results in a trivial state. We find that the $\text{In}_2\text{Se}_3/\text{In}_2\text{Te}_3$ bilayer of the DD configuration is such a case: the Wilson loop calculation confirms that the band topology (see the band structure in Fig. 4a) is trivial. Interestingly, by placing a monolayer Al right next to the Q^- surface (Fig. 4b), we recover a topologically nontrivial state with a decent band gap of ≈ 40 meV around Γ , and the corresponding topological edge states are shown in Fig. 4c. We attribute the enhancement of the band gap to the stronger hybridization between the Te-5p and Se-4p bands. The Se bands split by Al atoms have a large overlap with the Te 5p bands in energy, consequently leading to a stronger hybridization. Layer-resolved density of states further corroborates the reduction of built-in field within the $\text{In}_2\text{Se}_3/\text{In}_2\text{Te}_3$ bilayer because of the proximity effect of monolayer Al (see more details in Section VI, ESI†). The induced \mathbb{Z}_2 nontrivial topological edge states by Al coating pose a plausible scenario at low temperatures when Al turns superconducting.⁴³ The superconductivity proximitized edge states effectively realize a topological superconductor⁴⁴ that may host Majorana zero modes if terminated by a magnetic gap introduced either by an external in-plane magnetic field or by contact to certain magnetic materials. It is noted that the switchability of bilayer heterostructures such as $\text{In}_2\text{Se}_3/\text{In}_2\text{Te}_3$ is confirmed by computing the minimum energy pathways (see Section IX, ESI†).

The 2DFETIs exhibit a few features distinct from their 3D counterparts. First, a 2DFETI is expected to possess more

robust switchability than a 3DFETI. The conducting surface states of a 3DFETI, though in principle can serve as innate metallic electrodes to stabilize ferroelectricity at the nanoscale,²⁴ may also screen strongly the external electric field, hindering the polarization reversal process. In contrast, a 2DFETI behaves like a normal insulator along the out-of-plane direction, making it easier to switch P_{OP} . Because the band topology is strongly coupled with the direction and magnitude of P_{OP} , it is feasible to use an external electric field to drive a trivial-nontrivial topological phase transition, corresponding to an OFF–ON switch of the quantized edge conductance. According to our design principle (eqn (2)), the UU and DD configurations of a bilayer heterostructure can have different band topologies. Unlike $1\text{T}'\text{-MoS}_2$ that requires a sustained electric field to maintain the trivial state,³ the UU and DD configurations are intrinsically stable in the absence of an electric field, allowing non-volatile topological field-effect transistors. Additionally, the 180° domain wall (DW) separating UU and DD domains will support helical metallic states protected from back-scattering. These DWs in 2DFETI can serve as field-configurable and moveable quasi-1D dissipationless charge/spin transport channels (Fig. 5a), offering new opportunities of domain-wall-based quantum electrical circuits.⁴⁵

Finally, we propose a topological memristor (illustrated in Fig. 5b) for non-volatile multi-state applications based on vdW heterostructures of 2DFETIs separated by 2D wide-band-gap insulators such as hexagonal boron nitride (hBN). The device setup is similar to a topological transistor³ but with the advantages of being nonvolatile and multistate. Note that a

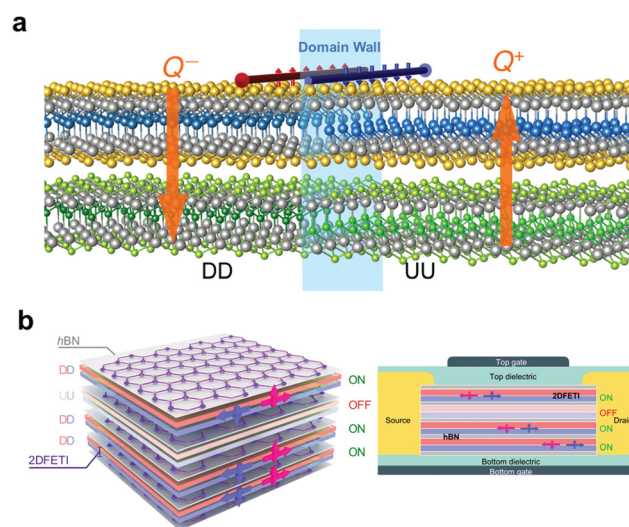


Fig. 5 Schematic diagram of 2DFETI-based devices. A hetero-bilayer is topologically trivial in the UU configuration and non-trivial in the DD configuration. (a) Ferroelectric domain walls as field-configurable and moveable quasi-1D channels carrying dissipationless spin current. (b) A non-volatile topological memristor made up of heterobilayers. The UU configuration is trivial and the DD configuration is nontrivial. The edge conductance can be written to any value between 0 and $2Ne^2/h$ for a stacked structure containing N layers of type-II 2DFETIs. The edge states remain nonvolatile in the absence of vertical electric fields between top and bottom gates.

field-effect transistor made completely from 2D materials has already been demonstrated,⁴⁶ indicating the possibility of constructing a similar unit using only 2D materials. The hetero-bilayer-based 2DFETI is topologically trivial in the UU configuration while non-trivial in the DD configuration. It has been demonstrated in ferroelectric thin films that the polarization state can be deterministically set to a desired value in an on-demand fashion by controlling the voltage and width of pulsed electric fields.^{47,48} Following a similar spirit, the edge conductance of the vdW heterostructure containing N sheets of 2DFETIs can be written electrically to any value between 0 and $2Ne^2/h$ by varying the number of bilayers of DD configurations, and retain the value without bias. The proposed 2DFETI-based topological memristor, combining the advantages of topological insulators, ferroelectrics, and two-dimensional materials, may hold promise for energy-efficient, high-density synaptic electronics and neuromorphic systems.

In summary, we develop a strategy to realize a novel class of quantum materials, type-II two-dimensional ferroelectric topological insulators, characterized with a direct coupling between band topology and polarization state. The design principle, supported by first-principles calculations with hybrid functionals, can be succinctly summarized as one equation that depends only on three material parameters: the out-of-plane polarization, work function, and electron affinity. The ability to construct topological quantum materials using only trivial building blocks, combined with the voltage-switchable quantized edge conductance, offers exciting opportunities for 2DFETI-based quantum electronics. A plausible combination of superconducting 2D materials and 2DFETI not only introduces nontrivial topological properties in the normal state but also likely provides a controllable topological superconductivity platform.

J. H., X. D., and S. L. acknowledge support from the National Natural Science Foundation of China (52002335), Westlake Education Foundation, and Westlake Multidisciplinary Research Initiative Center. Y. K. acknowledges support from the NRF Grant (2021R1A2C101387112). The computational resources were provided by Westlake HPC Center and the Korea Institute of Science and Technology Information (KISTI-KSC-2020-CRE-0108).

Conflicts of interest

There are no conflicts to declare.

References

- 1 K. S. Novoselov, Electric Field effect in atomically thin carbon Films, *Science*, 2004, **306**, 666.
- 2 C. L. Kane and E. J. Mele, Quantum spin hall effect in graphene, *Phys. Rev. Lett.*, 2005, **95**, 226801.
- 3 X. Qian, J. Liu, L. Fu and J. Li, Quantum spin hall effect in two-dimensional transition metal dichalcogenides, *Science*, 2014, **346**, 1344.
- 4 L. Kou, Y. Ma, Z. Sun, T. Heine and C. Chen, Two-dimensional topological insulators: Progress and prospects, *J. Phys. Chem. Lett.*, 2017, **8**, 1905.
- 5 A. Marrazzo, M. Gibertini, D. Campi, N. Mounet and N. Marzari, Relative abundance of Z2 topological order in exfoliable two-dimensional insulators, *Nano Lett.*, 2019, **19**, 8431.
- 6 A. Marrazzo, M. Gibertini, D. Campi, N. Mounet and N. Marzari, Prediction of a large-gap and switchable kane-mele quantum spin hall insulator, *Phys. Rev. Lett.*, 2018, **120**, 117701.
- 7 I. P. Batra, P. Wurfel and B. D. Silverman, Phase transition, stability, and depolarization Field in ferroelectric thin Films, *Phys. Rev. B: Solid State*, 1973, **8**, 3257.
- 8 A. Belianinov, Q. He, A. Dziazgys, P. Maksymovych, E. Eliseev, A. Borisevich, A. Morozovska, J. Banys, Y. Vysochanskii and S. V. Kalinin, CuInP₂S₆ room temperature layered ferroelectric, *Nano Lett.*, 2015, **15**, 3808.
- 9 Y. Zhou, D. Wu, Y. Zhu, Y. Cho, Q. He, X. Yang, K. Herrera, Z. Chu, Y. Han, M. C. Downer, H. Peng and K. Lai, Out-of-plane piezoelectricity and ferroelectricity in layered α -In₂Se₃ nano akes, *Nano Lett.*, 2017, **17**, 5508.
- 10 K. Chang, J. Liu, H. Lin, N. Wang, K. Zhao, A. Zhang, F. Jin, Y. Zhong, X. Hu and W. Duan, *et al.*, Discovery of robust in-plane ferroelectricity in atomic-thick SnTe, *Science*, 2016, **353**, 274.
- 11 S. Yuan, X. Luo, H. L. Chan, C. Xiao, Y. Dai, M. Xie and J. Hao, Room-temperature ferroelectricity in MoTe₂ down to the atomic monolayer limit, *Nat. Commun.*, 2019, **10**, 1175.
- 12 J. Xiao, Y. Wang, H. Wang, C. D. Pemmaraju, S. Wang, P. Muscher, E. J. Sie, C. M. Nyby, T. P. Devereaux, X. Qian, X. Zhang and A. M. Lindenberg, Berry curvature memory through electrically driven stacking transitions, *Nat. Phys.*, 2020, **16**, 1028.
- 13 W. Ding, J. Zhu, Z. Wang, Y. Gao, D. Xiao, Y. Gu, Z. Zhang and W. Zhu, Prediction of intrinsic two-dimensional ferroelectrics in In₂Se₃ and other III₂-VI₃ van der Waals materials, *Nat. Commun.*, 2017, **8**, 14956.
- 14 D. L. Duong, S. J. Yun and Y. H. Lee, van der Waals layered materials: Opportunities and challenges, *ACS Nano*, 2017, **11**, 11803.
- 15 X. Zou, Y. Xu and W. Duan, 2d materials: Rising star for future applications, *Innovation*, 2021, **2**, 100115.
- 16 R. Peng, Y. Ma, S. Zhang, B. Huang, L. Kou and Y. Dai, Self-doped p-n junctions in twodimensional In₂Se₃ van der Waals materials, *Mater. Horiz.*, 2020, **7**, 504.
- 17 L. Kou, H. Fu, Y. Ma, B. Yan, T. Liao, A. Du and C. Chen, Two-dimensional ferroelectric topological insulators in functionalized atomically thin bismuth layers, *Phys. Rev. B*, 2018, **97**, 075429.
- 18 X. Kai Hu, Z. Xia Pang, C. Wen Zhang, P. Ji Wang, P. Li and W. Xiao Ji, A two-dimensional robust topological insulator with coexisting ferroelectric and valley polarization, *J. Mater. Chem. C*, 2019, **7**, 9406.
- 19 J.-J. Zhang, D. Zhu and B. I. Yakobson, Heterobilayer with ferroelectric switching of topological state, *Nano Lett.*, 2020, **21**, 785.

- 20 H. Bai, X. Wang, W. Wu, P. He, Z. Xu, S. A. Yang and Y. Lu, Nonvolatile ferroelectric control of topological states in two-dimensional heterostructures, *Phys. Rev. B*, 2020, **102**, 235403.
- 21 Y. Liang, N. Mao, Y. Dai, L. Kou, B. Huang and Y. Ma, Intertwined ferroelectricity and topological state in two-dimensional multilayer, 2021, arXiv: 2102.07294.
- 22 D. Khomskii, Classifying multiferroics: Mechanisms and effects, *Physics*, 2009, **2**, 20.
- 23 C. Lu, M. Wu, L. Lin and J.-M. Liu, Single-phase multiferroics: new materials, phenomena, and physics, *Natl. Sci. Rev.*, 2019, **6**, 653.
- 24 S. Liu, Y. Kim, L. Z. Tan and A. M. Rappe, Strain-induced ferroelectric topological insulator, *Nano Lett.*, 2016, **16**, 1663.
- 25 T. Sluka, A. K. Tagantsev, D. Damjanovic, M. Gureev and N. Setter, Enhanced electromechanical response of ferroelectrics due to charged domain walls, *Nat. Commun.*, 2012, **3**, 748.
- 26 J. von Neumann and E. Wigner, No crossing rule, *Phys. Z.*, 1927, **30**, 467.
- 27 N. Mounet, M. Gibertini, P. Schwaller, D. Campi, A. Merkys, A. Marrazzo, T. Sohier, I. E. Castelli, A. Cepellotti and G. Pizzi, *et al.*, Two-dimensional materials from high-throughput computational exfoliation of experimentally known compounds, *Nat. Nanotechnol.*, 2018, **13**, 246.
- 28 B. Luo, Y. Yao, E. Tian, H. Song, X. Wang, G. Li, K. Xi, B. Li, H. Song and L. Li, Graphenelike monolayer monoxides and monochlorides, *Proc. Natl. Acad. Sci. U. S. A.*, 2019, **116**, 17213.
- 29 S. Gupta, A. Kutana and B. I. Yakobson, Heterobilayers of 2D materials as a platform for excitonic superfluidity, *Nat. Commun.*, 2020, **11**, 2989.
- 30 C. Cui, W.-J. Hu, X. Yan, C. Addiego, W. Gao, Y. Wang, Z. Wang, L. Li, Y. Cheng, P. Li, X. Zhang, H. N. Alshareef, T. Wu, W. Zhu, X. Pan and L.-J. Li, Intercorrelated in-plane and out-of-plane ferroelectricity in ultrathin two-dimensional layered semiconductor In_2Se_3 , *Nano Lett.*, 2018, **18**, 1253.
- 31 F. Xue, J. Zhang, W. Hu, W.-T. Hsu, A. Han, S.-F. Leung, J.-K. Huang, Y. Wan, S. Liu, J. Zhang, J.-H. He, W.-H. Chang, Z. L. Wang, X. Zhang and L.-J. Li, Multidirection piezoelectricity in mono- and multilayered hexagonal $\alpha\text{-In}_2\text{Se}_3$, *ACS Nano*, 2018, **12**, 4976.
- 32 S. Wan, Y. Li, W. Li, X. Mao, C. Wang, C. Chen, J. Dong, A. Nie, J. Xiang, Z. Liu, W. Zhu and H. Zeng, Nonvolatile ferroelectric memory effect in ultrathin $\alpha\text{-In}_2\text{Se}_3$, *Adv. Funct. Mater.*, 2019, **29**, 1808606.
- 33 Y. Zhang, X. Tang, W. Wang, L. Jin and G. Li, Large-size ultrathin $\alpha\text{-Ga}_2\text{S}_3$ nanosheets toward high-performance photodetection, *Adv. Funct. Mater.*, 2021, **31**, 2008307.
- 34 O. I. Malyi, K. V. Sopiha and C. Persson, Energy, phonon, and dynamic stability criteria of two-dimensional materials, *ACS Appl. Mater. Interfaces*, 2019, **11**, 24876.
- 35 L. Li and M. Wu, Binary compound bilayer and multilayer with vertical polarizations: Two-dimensional ferroelectrics, multiferroics, and nanogenerators, *ACS Nano*, 2017, **11**, 6382.
- 36 K. Yasuda, X. Wang, K. Watanabe, T. Taniguchi and P. Jarillo-Herrero, Stacking-engineered ferroelectricity in bilayer boron nitride, *Science*, 2021, **372**, 1458.
- 37 M. V. Stern, Y. Waschitz, W. Cao, I. Nevo, K. Watanabe, T. Taniguchi, E. Sela, M. Urbakh, O. Hod and M. B. Shalom, Interfacial ferroelectricity by van der Waals sliding, *Science*, 2021, **372**, 1462.
- 38 P. Giannozzi, S. Baroni, N. Bonini, M. Calandra, R. Car, C. Cavazzoni, D. Ceresoli, G. L. Chiarotti, M. Cococcioni and I. Dabo, *et al.*, QUANTUM ESPRESSO: a modular and open-source software project for quantum simulations of materials, *J. Phys.: Condens. Matter*, 2009, **21**, 395502.
- 39 P. Giannozzi, O. Andreussi, T. Brumme, O. Bunau, M. B. Nardelli, M. Calandra, R. Car, C. Cavazzoni, D. Ceresoli and M. Cococcioni, *et al.*, Advanced capabilities for materials modelling with QUANTUM ESPRESSO, *J. Phys.: Condens. Matter*, 2017, **29**, 465901.
- 40 A. V. Krugau, O. A. Vydrov, A. F. Izmaylov and G. E. Scuseria, Influence of the exchange screening parameter on the performance of screened hybrid functionals, *J. Chem. Phys.*, 2006, **125**, 224106.
- 41 N. Marzari, A. A. Mostofi, J. R. Yates, I. Souza and D. Vanderbilt, Maximally localized wannier functions: Theory and applications, *Rev. Mod. Phys.*, 2012, **84**, 1419.
- 42 G. Pizzi, V. Vitale, R. Arita, S. Blügel, F. Freimuth, G. Géranton, M. Gibertini, D. Gresch, C. Johnson, T. Koretsune, J. Ibañez-Azpiroz, H. Lee, J.-M. Lihm, D. Marchand, A. Marrazzo, Y. Mokrousov, J. I. Mustafa, Y. Nohara, Y. Nomura, L. Paulatto, S. Poncé, T. Ponweiser, J. Qiao, F. Thöle, S. S. Tsirkin, M. Wierzbowska, N. Marzari, D. Vanderbilt, I. Souza, A. A. Mostofi and J. R. Yates, Wannier90 as a community code: new features and applications, *J. Phys.: Condens. Matter*, 2020, **32**, 165902.
- 43 R. Meservey and P. M. Tedrow, Properties of very thin aluminum films, *J. Appl. Phys.*, 1971, **42**, 51.
- 44 J. Nilsson, A. R. Akhmerov and C. W. J. Beenakker, Splitting of a Cooper pair by a pair of Majorana bound states, *Phys. Rev. Lett.*, 2008, **101**, 120403.
- 45 G. F. Nataf, M. Guennou, J. M. Gregg, D. Meier, J. Hlinka, E. K. H. Salje and J. Kreisel, Domain-wall engineering and topological defects in ferroelectric and ferroelastic materials, *Nat. Rev. Phys.*, 2020, **2**, 634.
- 46 T. Roy, M. Tosun, J. S. Kang, A. B. Sachid, S. B. Desai, M. Hettick, C. C. Hu and A. Javey, Field-effect transistors built from all two-dimensional material components, *ACS Nano*, 2014, **8**, 6259.
- 47 A. Chanthbouala, V. Garcia, R. O. Cherifi, K. Bouzouane, S. Fusil, X. Moya, S. Xavier, H. Yamada, C. Deranlot, N. D. Mathur, M. Bibes and A. Barth, élém, and J. Grollier, A ferroelectric memristor, *Nat. Mater.*, 2012, **11**, 860.
- 48 R. Xu, S. Liu, S. Saremi, R. Gao, J. J. Wang, Z. Hong, H. Lu, A. Ghosh, S. Pandya, E. Bonturim, Z. H. Chen, L. Q. Chen, A. M. Rappe and L. W. Martin, Kinetic control of tunable multi-state switching in ferroelectric thin films, *Nat. Commun.*, 2019, **10**, 1282.
- 49 L. Bengtsson, Dipole correction for surface supercell calculations, *Phys. Rev. B: Condens. Matter Mater. Phys.*, 1999, **59**, 12301.